Environmental Science & Technology

Article

Cite This: Environ. Sci. Technol. XXXX, XXX, XXX−XXX

pubs.acs.org/est

# Hypoxia Causes Transgenerational Impairment of Ovarian Development and Hatching Success in Fish

Keng Po Lai,[^,†,⊥] Simon Yuan Wang,[^,■,△] Jing Woei Li,[†] Yin Tong,[‡] Ting Fung Chan,[§,∥] Nana Jin,[§] Anna Tse,[‡] Jiang Wen Zhang,[‡] Miles Teng Wan,[†] Nathan Tam,[†] Doris Wai Ting Au,[†,⊥] Bo-Young Lee,[○] Jae-Seong Lee,[○] Alice Sze Tsai Wong,[‡] Richard Yuen Chong Kong,[†,⊥] and Rudolf Shiu Sun Wu[*,⊥,#]

[†]Department of Chemistry, The City University of Hong Kong, Hong Kong SAR, China

[‡]School of Biological Sciences, The University of Hong Kong, Hong Kong SAR, China

[§]School of Life Sciences, The Chinese University of Hong Kong, Hong Kong SAR, China

[∥]Partner State Key Laboratory of Agrobiotechnology, The Chinese University of Hong Kong, Hong Kong SAR, China

[⊥]State Key Laboratory of Marine Pollution, The City University of Hong Kong, Hong Kong SAR, China

[#]Department of Science and Environmental Studies, The Education University of Hong Kong, Hong Kong SAR, China

[○]Department of Biological Science, College of Science, Sungkyunkwan University, Suwon, South Korea

[■]Division of Newborn Medicine, Children's Hospital Boston, 300 Longwood Avenue, Boston, Massachusetts 02115, United States

[△]Department of Pediatrics, Harvard Medical School, Boston, Massachusetts 02115, United States

Supporting Information

**ABSTRACT:** Hypoxia is a pressing environmental problem in both marine and freshwater ecosystems globally, and this problem will be further exacerbated by global warming in the coming decades. Recently, we reported that hypoxia can cause transgenerational impairment of sperm quality and quantity in fish (in F0, F1, and F2 generations) through DNA methylome modifications. Here, we provide evidence that female fish (*Oryzias melastigma*) exposed to hypoxia exhibit reproductive impairments (follicle atresia and retarded oocyte development), leading to a drastic reduction in hatching success in the F2 generation of the transgenerational group, although they have never been exposed to hypoxia. Further analyses show that the observed transgenerational impairments in ovarian functions are related to changes in the DNA methylation and expression pattern of two gene clusters that are closely associated with stress-induced cell cycle arrest and cell apoptosis. The observed epigenetic and transgenerational alterations suggest that hypoxia may pose a significant threat to the sustainability of natural fish populations.

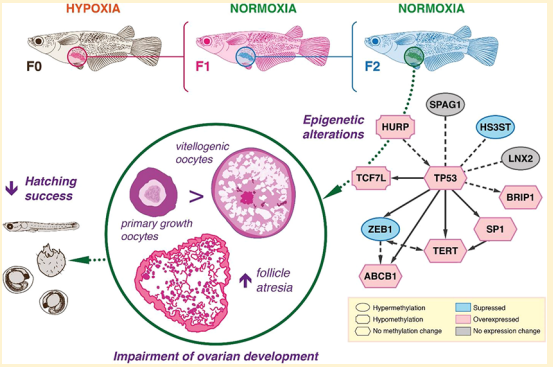


## INTRODUCTION

Hypoxia is a pressing environmental problem in aquatic ecosystems, and over 400 "dead zones" [with <2 mg/L dissolved oxygen (DO)] have been identified in coastal waters worldwide.[1] The impending problem of global warming will further exacerbate the problem by reducing oxygen solubility and increasing water stratification and biological oxygen demand.[2] It is predicted that 94% of dead zones will experience at least a 2 °C temperature increase by the end of the century.[3] Previous laboratory and field studies have shown that hypoxia is an endocrine disruptor that impairs the reproduction of fish, amphibians, and mammals[4−6] through deregulation of steroidogenesis at both the molecular and cellular levels.[5,7,8] Hypoxia is also a teratogen that leads to the malformation of F1-generation fish by altering apoptosis.[9] Recently, we discovered that hypoxia can cause transgenerational impairment of sperm quality and quantity in fish (in F0, F1, and F2) through DNA methylome modifications.[6] These epigenetic changes associated with transgenerational reproductive impairments are concordant with the hypothesis of "transgenerational stress inheritance", in which parental exposure to stress or environmental changes can lead to adverse effects on offspring through epigenetic changes.[10,11] Almost all studies on transgenerational impairments are limited to males. For example, vinclozolin has been shown to decrease spermatogenesis and increase male infertility in the F1 to Fv4 generations.[12] In another study, differential histone modifica-

Received: December 26, 2018
Revised: March 5, 2019
Accepted: March 7, 2019
Published: March 7, 2019






DOI: 10.1021/acs.est.8b07250
Environ. Sci. Technol. XXXX, XXX, XXX−XXX

tions were found in the F3 generation of rats, when F0 was exposed to vinclozolin and dichlorodiphenyltrichloroethane.[13] Only one study provided evidence that polychlorinated biphenyls could exert transgenerational effects (changes in sex hormone levels) on F2 and F3 female rats,[14] and transgenerational effects through female germlines and reproductive impairment have so far not been demonstrated yet. Using the marine medaka (*Oryzias melastigma*) as a model, we tested the hypothesis that hypoxia could cause transgenerational reproductive impairment in females. Phenotypic, transcriptomic, bioinformatic, and methylomic analyses were conducted to elucidate possible epigenetic mechanisms leading to the observed transgenerational impairment caused by hypoxia.

## METHODS

**Experimental Design.** Marine medaka (*Oryzias melastigma*) were maintained under optimal growth and breeding conditions (5.8 mg $O_2$/L, 28 ± 2 °C, pH 7.2 in a 14-h light:10-h dark cycle). The experimental design for the normoxia, hypoxia, and transgenerational groups followed the protocols described in our previous study.[6] Briefly, marine medaka (F0) were exposed to normoxia (5.8 ± 0.2 mg $O_2$/L; equivalent to 78% $PO_2$) (F0N) or hypoxia (1.5 ± 0.2 mg $O_2$/L; equivalent to 15−20% $PO_2$) (F0H) for 1 mo. The desired level of dissolved oxygen (DO) was achieved by bubbling a constant flow of premixed air and nitrogen into a 300-L reservoir tank through a stripping column (diameter = 4 cm), and the DO was monitored twice daily using a DO meter (YSI model 580). Water temperature was controlled by placing the fish tanks in an environmental chamber and monitored daily using a thermometer. Salinity was monitored using a NuLine salinity tester three times per week. pH and ammonia level were measured using a pH meter and an API aquarium ammonia test kit, respectively, once per week. One-third of the water was changed weekly, and the oxygen level was maintained at the desired level using a continuous gas supply. To avoid direct effects on germ cells, embryos produced by F0 were collected within 1 h postfertilization before the appearance of primordial germ cells.[15] Embryos were immediately transferred to normoxic or hypoxic conditions for the development of the F1 generation. The F1 generations of the normoxic (F1N) and hypoxic (F1H) groups were kept under the same conditions as the F0 generation to produce the F2 generation (F2N normoxic group and F2H hypoxic group). Half of the F0H fish were returned to normoxia (F0T) to produce the transgenerational group for the following two generations (F1T and F2T) (Figure 1). Each of the above treatment consisted of five replicate net cages (52 cm length × 18 cm width × 27.5 cm height), and each cage contained 45 male and 45 female medaka fish.

**Hatching Success.** In each treatment, three cages were randomly selected, and 100 embryos were randomly sampled from each cage at day 10 after fertilization. Hatching success in each replicate cage (expressed as percentage of hatched embryos) was determined.

**RNA and DNA Isolation.** After the normoxic/hypoxic/transgenerational treatment, fish were anesthetized in an ice bath. Ovary tissues were dissected from female fish ($n$ = 30) randomly selected from the F0, F1, and F2 generations of each treatment group. Three ovaries from the same treatment group were pooled to produce one RNA sample. Another three ovaries from the same treatment group were pooled to prepare

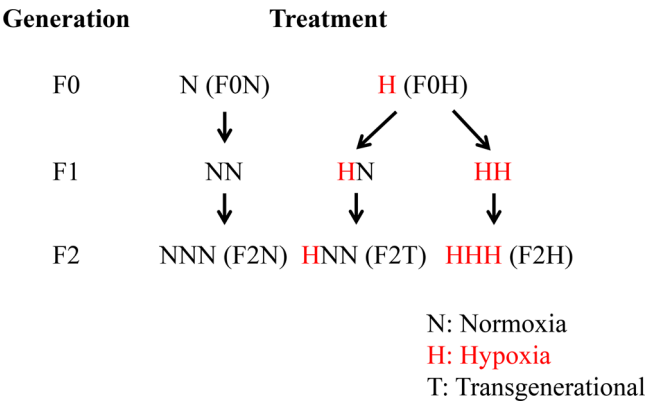


**Figure 1.** Experimental setup.

the corresponding DNA sample. Three replicates of pooled RNA/DNA samples (representing 9 individual fish) from each exposure condition and generation (i.e., normoxia control (F0N) and hypoxia (F0H) treatment in the F0 generation, along with normoxia (F2N), hypoxia (F2H), and transgenerational (F2T) groups in the F2 generation) were prepared. Total RNA was extracted from tissue samples using the mirVana RNA isolation kit (Applied Biosystems) according to the manufacturer's instructions. Briefly, ovaries were lysed in 500 μL of lysis/binding buffer and incubated on ice for 10 min. Then, 500 μL of acid phenol:chloroform was added, and the sample was centrifuged at 10 000$g$ for 5 min. Next, 400 uL of the aqueous phase was mixed with 500 uL of 100% ethanol. The mixture was loaded onto the filter cartridge and centrifuged at 10 000$g$ for 15 s. The filter cartridge was then washed with wash solution, and the RNA was eluted by the addition of 60 μL of preheated 95 °C water to the filter cartridge and centrifugation at 10000$g$ for 20 s. RNA quality was assessed using an Agilent 2100 Bioanalyzer system, and samples with an RNA integrity number (RIN) greater than eight were used for RNA library construction. For DNA isolation, a DNeasy Blood & Tissue Kit (Qiagen) was utilized according to the manufacturer's instructions. Briefly, the pooled samples were homogenized in 360 μL of Buffer ATL using a pellet pestle. Then, 40 μL of proteinase K was added to the homogenized samples and incubated at 56 °C overnight. Endogenous RNA in the sample was degraded with RNase A. Then, 400 μL of buffer AL and 400 μL of the 100% ethanol mixture were added to the sample, followed by vortexing for 10 s. DNA was concentrated using a DNeasy Mini spin column.

**RNA Sequencing and Bioinformatics Analysis.** Fifteen RNA (cDNA) libraries (three biological replicates from each condition in the F0 and F2 generations; represented nine individuals in each condition) of ovaries were constructed. The libraries were sequenced by the Beijing Genomics Institute (Wuhan, China). Single-end 50-bp read-length reads were sequenced on a BGISEQ-500RS sequencer. Sequence reads were, in turn, dynamically trimmed according to BWA's −q algorithm.[6] At least 48 million quality-trimmed reads were obtained in each sample (Supplementary Data Set S6). Quality-trimmed sequence reads were quantified against the *Oryzias melastigma* transcriptome assembly[16] using Kallisto version 0.43.0.[17] Read-count data were then subjected to differential expression analysis using the edgeR package.[18] Genes with |log2 (fold change: treatment/control)| > 1, log2 CPM > 0, and $p$ < 0.05 were considered differentially expressed genes (DEGs). Furthermore, ingenuity pathway


DOI: 10.1021/acs.est.8b07250
Environ. Sci. Technol. XXXX, XXX, XXX−XXX

analysis (IPA, QIAGEN, www.qiagen.com/ingenuity) was used to decipher the transgenerational effect of hypoxia on ovarian function. In the bioinformatics analysis, all pathways, diseases or biofunctions with $p < 0.05$ were considered statistically significant.

**Reduced Representation Bisulfite Sequencing (RRBS).** Genomic DNA (2 μg per sample) was digested overnight with 64 units of *MspI* (NEB). Digested DNA was purified using the QIAquick nucleotide removal kit (Qiagen). End-repair, A-tailing at the 3′ end, and methylated indexed adapter ligation at the terminal ends were performed using the KAPA Hyper prep kit (KAPABiosystems) and SeqCap adapter kits (Roche). After library purification with AMPure beads (Beckman), library sizes ranging from 150 to 350 bp (30−230 bp of MspI digested DNA plus 120 bp of adapters) were excised using BluePippin with 3% agarose gel cassette (Marker Q3). Size-selected libraries were treated with an EZ DNA Methylation-Lightning Kit (Zymo Research) for bisulfite conversion. To amplify the bisulfite-converted libraries, PfuTurbo Cx Hotstart DNA Polymerase (Agilent) and Library Amplification Primer Mix (KAPABiosystems) were utilized for 12 cycles of amplification. The library quality was assessed using a high-sensitivity DNA assay on the 2100 Bioanalyzer system (Agilent), and the library quantity was assessed with a Qubit dsDNA high-sensitivity assay (Life Technologies). The libraries were denatured, diluted to optimal concentrations, and then used in the cluster generation steps. A HiSeq PE Cluster Kit v4 with cbot was used for cluster generation on the flow cell. An Illumina HiSeq SBS Kit v4 was utilized for pair-end 101 bp sequencing. Library preparation and Illumina sequencing (pair-end sequencing of 101 bp) were performed at the University of Hong Kong, Centre for Genomic Sciences (HKU, CGS). A total throughput of 26.6 Gb was obtained (Table 1). In terms of sequence quality, an average of 87% of the bases achieved a quality score of Q30, where Q30 denotes the accuracy of a base call to be 99.9%.

**Table 1. Distribution of Throughput for Each Sample in RRBS**

| sample | number of raw reads | total throughput (Gb) | % of ≥ Q30 bases |
|---|---|---|---|
| F0N | 56094182 | 5.7 | 88 |
| F0H | 46169646 | 4.7 | 87 |
| F2N | 54003838 | 5.5 | 89 |
| F2H | 50293168 | 5.1 | 87 |
| F2T | 56544442 | 5.7 | 85 |

**RRBS Data Analysis.** The raw fastq files were quality filtered and trimmed by using wrapper script, TrimGalore 0.4.3, and paired with Cutadapt 1.9.1 in pair-end mode.[19,20] The bisulfite genome was prepared by Bismark Genome Preparation (0.19.0) from the genome of the marine medaka *Oryzias melastigma* (Om v0.7 RACA genomic). Next, we constructed a sequence alignment of the RRBS sequences against the medaka bisulfite genome by Bismark with Bowtie 2, and an average of 67% of sequences were successfully mapped on the genome. The alignment results were then analyzed using the methylation extractor in Bismark, and on average a total of 62 073 143 CpGs were covered in the RRBS sequencing result, of which approximately 69% were methylated at the genome-wide level (Supplementary Data Set S7). Methylation data were filtered and normalized with the Biseq package in R. We generated differential methylation data for each CpG to locate the differentially methylated regions (DMRs) (minimum median beta difference 0.1, maximum length 50 bp). Finally, each DMR was mapped to the coding genes on the reference genome, and hyper- and hypo-methylated genes were detected based on the methylation levels of their promoters (TSS ± 2000 bp).

**cDNA Synthesis and Gene Expression Analysis.** Total RNA from eight ovaries from each condition of the F0, F1, and F2 generations was converted to cDNAs using the SuperScript VILO cDNA synthesis kit. Expression of each target gene was determined using quantitative polymerase chain reaction (qPCR). The gene-specific primers are listed in Supplementary Data Set S8. Emission intensity was detected with the StepOne real-time PCR system (Applied Biosystems). To adjust for variations in the amount of starting template, gene expression was normalized against the 18S rRNA.

**Haematoxylin and Eosin (H&E) Staining.** Whole medaka fish were anesthetized in ice−water, followed by flushing with GPHS fixative (0.05% glutaraldehyde−2% paraformaldehyde−80% HistoChoice containing 1% sucrose and 1% $CaCl_2$) through the mouth, gills, and abdominal cavity. After removal of the skull roof, othliths, and fins with a scalpel, a small hole was punched into the swim bladder to release the air within. The medaka were immersed in fixative for 24 h and then dehydrated in a graded series of methanol (70%, 80%, 95% × 2, 100% × 3) for 20 min per step, followed by rinsing with chloroform three times (30 min each). The medaka were then infiltrated and embedded in paraffin.[21] Paraffin sections (5-μm thick) of fish were cut using a microtome (Leica) and placed on glass slides. The paraffin was removed by immersing the slides in xylenes (5 min × 3). After deparaffinization, tissue sections were rehydrated using a graded ethanol series (100% × 2, 95%, and 70%). Slides were stained with Mayer's hematoxylin (Sigma-Aldrich) and eosin (Sigma-Aldrich). Color was enhanced by 1% acid ethanol and 0.2% ammonia−water. Another graded ethanol series (95% × 2, 100% × 3) was used to dehydrate tissue on slides. After dehydration, the slides were rinsed with xylene and mounted in toluene solution (Fisher Chemicals). The sections were examined and photographed at magnifications of 20× and 200× with a light microscope (Nikon Eclipse 90i) equipped with a digital imaging system (SPOT 4.6).

**Examination of Follicle Atresia and Oocyte Staging.** Atresia, a degenerative and resorptive process during oogenesis, is characterized by an increase in size of follicular cells and breakdown of chorion.[22] Ovarian development is divided into three major phases characterized by primary growth oocytes, vitellogenic oocytes, and mature oocytes.[22] Oocyte staging was quantified following the method of Kinoshita et al.[23] Briefly, the primary growth phase is concomitant with oocyte growth, and multiple nucleoli are present at the periphery of the nucleus. Vitellogenic oocytes are characterized by the centralized appearance of spherical, vitellogenic yolk globules and the formation of a chorion. Mature oocytes have a hydrated, eosinophilic yolk mass that occupies most of the area of the oocyte. In the present study, H&E stained ovary sections were evaluated and quantified to assess the proportion of oocytes in each stage and the percentage of follicle atresia ($N$ = 8 in F0, $N$ = 6 in F1, and $N$ = 6 in F2). The number of oocytes in each phase on a slide section was counted under a light microscope (Nikon Eclipse 90i, 20× and 200× magnification), and the total number of oocytes was calculated. Three sections


DOI: 10.1021/acs.est.8b07250
Environ. Sci. Technol. XXXX, XXX, XXX−XXX

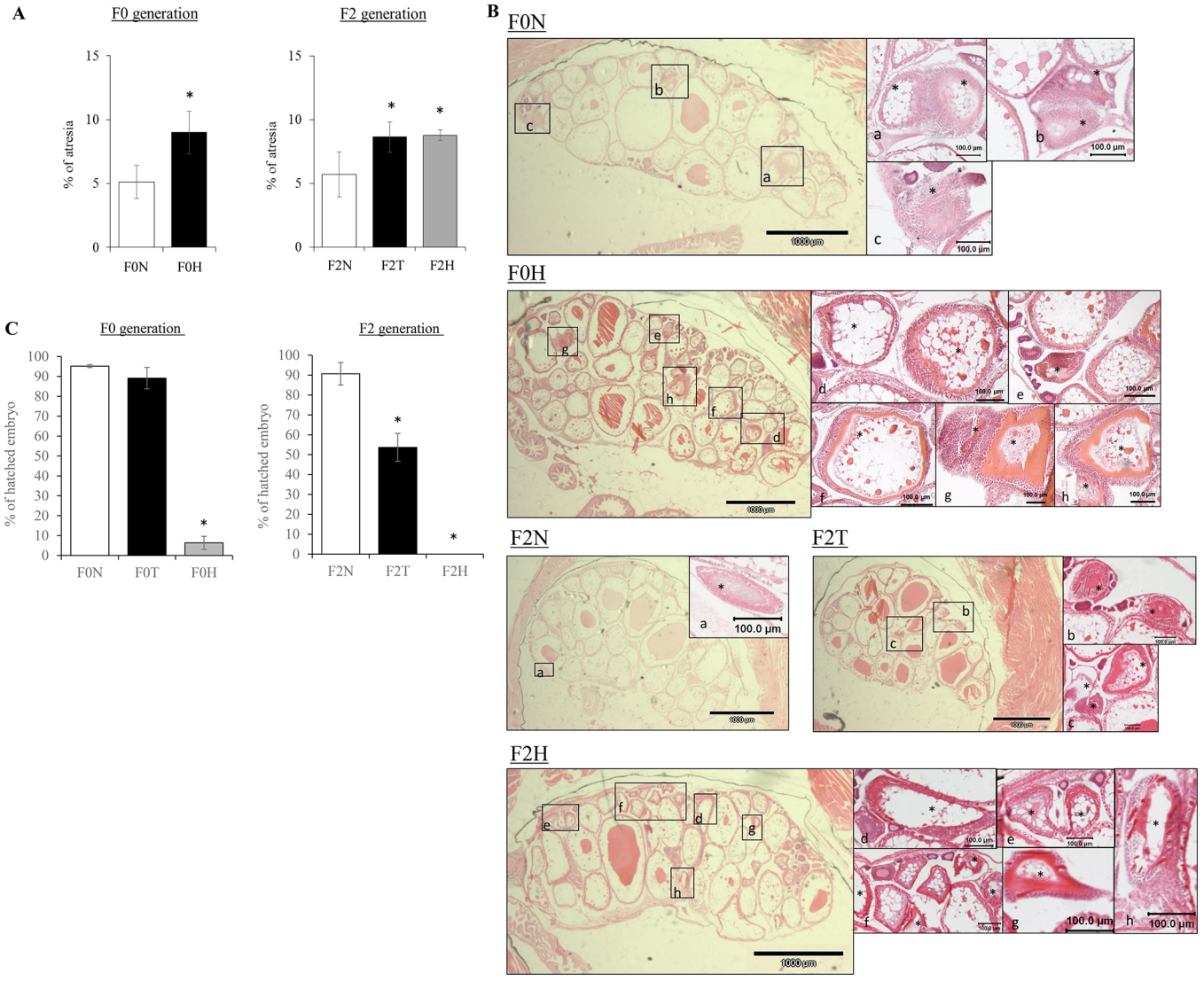


**Figure 2.** Transgenerational impairment of ovarian function in F0 and F2 generations. (**A**) Follicle atresia in F0 and F2 generations. N, T, and H represent normoxic, transgenerational, and hypoxic groups, respectively (F0, $n$ = 8; F2, $n$ = 7) (*$p$ < 0.05). (**B**) Representative histological images of hematoxylin and eosin staining in F0 and F2 generations. Follicle atresia is indicated with asterisks. (**C**) Effect of hypoxic exposure on 10-day hatchability in F1 and F3 embryos in the normoxic, transgenerational (F0T represents F0 fish that were exposed to hypoxia for 1 month and then transferred to and maintained under normoxia for the remaining period), and hypoxic groups ($n$ = 100 in each replicate). Data are presented as mean ± SEM. Asterisks denote statistically significant differences compared to the normoxic group (*$p$ < 0.05, $n$ = 3).

were assessed for each individual fish, with an interval of 20 sections between them.

**Statistical Analysis.** In the bioinformatics analysis, all pathways, diseases, or biofunctions with $p$ < 0.05 were considered statistically significant. In gene expression analysis and phenotypic analysis one-way analysis of variance (ANOVA) followed by LSD's *post hoc* test was performed to determine intergroup differences among F2N, F2T, and F2H. Student's $t$ test was used to identify significant difference between the F0N and F0H groups. All statistical analyses were performed using SPSS Statistics software, and a $p$-value of <0.05 was considered statistically significant.

## RESULTS

**Hypoxia Reduces the Hatching Success of Eggs in a Transgenerational Manner.** This study shows that exposure to hypoxia in F0 can alter ovarian functions and reduce the hatching success of eggs of both F0 and F2 females, despite the fact that the latter were never exposed to hypoxia. Induction of follicle atresia was clearly evident in the ovaries of F0 fish exposed to hypoxia (Figure 2A), as revealed by the increased size of follicular cells and chorion breakdown (Figure 2B). Additionally, there was a significantly greater proportion of primary growth oocytes and significantly fewer vitellogenic oocytes under hypoxia exposure (Supplementary Figure 1). Interestingly these adverse effects exhibited in F0 fish exposed to hypoxia were also found in the transgenerational F2T fish (Supplementary Figure 1), even though the fish were never exposed to hypoxia. Reproductive impairment was clearly evident in F0H fish, as clearly exemplified by a significant reduction in hatching success (Figure 2C). Importantly, such phenotypic change was also observed in both the transgenerational group (F2T) and hypoxic (F2H) groups (Figure 2C). Taken together, our results suggest that ancestral exposure to hypoxia could cause transgenerational reproductive impairment, decreasing the quality and hatching success of eggs.


DOI: 10.1021/acs.est.8b07250
Environ. Sci. Technol. XXXX, XXX, XXX−XXX

**Hypoxia Causes Transgenerational Differential Gene Expression in the Fish Ovary.** Transcriptomic analysis was performed to identify and compare differential gene expression between normoxic, hypoxic, and transgenerational groups. When comparing F0 fish of the hypoxic group (F0H) to F0 of the normoxic group (F0N) (Figure 3A), 683 differentially

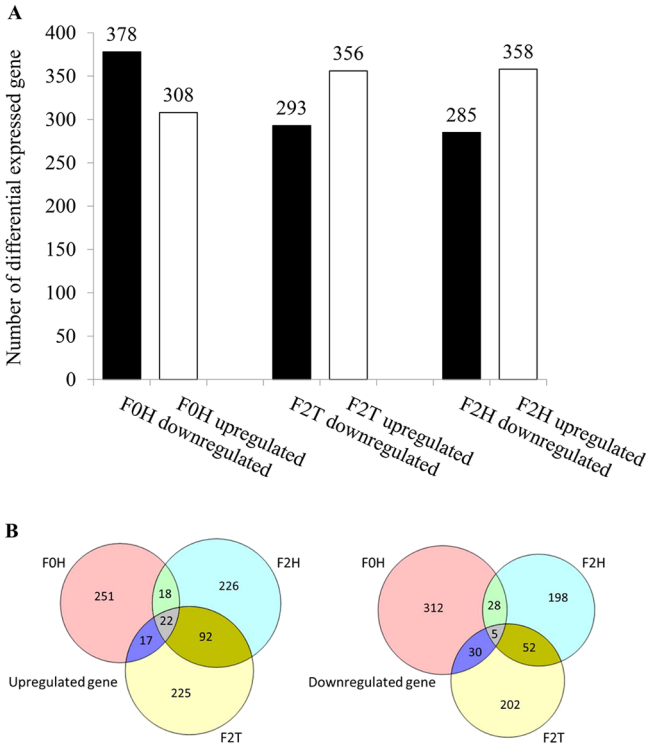


**Figure 3.** Hypoxia-induced differentially expressed genes (DEGs) in ovaries of F0 and F2 generations. (**A**) DEG statistics. The *X*-axis represents the names of comparable groups in various generations. The *Y*-axis represents the number of DEGs. (**B**) Venn diagram of overlapping significantly upregulated or downregulated genes shared among F0H_F0N, F2T_F2N, and F2H_F2N ($n$ = 9).

expressed genes (DEGs) were found, including 308 upregulated genes and 375 downregulated genes (Supplementary Data Set S1). In the F2 generation, we obtained 641 and 645 DEGs in the hypoxia group (F2H) (Supplementary Data Set S2) and transgenerational group (F2T), respectively (Supplementary Data Set S3), when compared to F2 of the normoxic group (F2N) (Figure 3A). When we compared the DEGs from the F0H, F2H, and F2T groups, 22 commonly upregulated genes and five downregulated genes were identified (Figure 3B).

**Hypoxia Induces Transgenerational Effects on Ovarian Function.** To understand the mechanism underlying the observed transgenerational effect of hypoxia on ovarian functions, the 645 DEGs in F2T were subjected to IPA. Canonical pathway analysis via IPA demonstrated that F2T showed significant interruption ($p < 0.05$) of a number of pathways related to cell cycle control and apoptosis (Figure 4A and Supplementary Data Set S4), including protein kinase A signaling, PEDF signaling, RhoA signaling, RhoGDI signaling, autophagy, the BER pathway, the role of BRCA1 in the DNA damage response, and death receptor signaling (Figure 4A and Supplementary Data Set S4). In addition to the pathways exhibiting significant effects ($p < 0.05$), alterations were found in important pathways controlling cell death (e.g., ATM signaling, telomerase signaling, apoptosis signaling, FAK signaling, and p53 signaling) in the F2T group (Supplementary Data Set S4). Similar alterations were identified in the IPA analysis of the 683 DEGs in the F0H group ($p < 0.01$) (Figure 4B and Supplementary Data Set S5), although the gene clusters were not completely identical (Table 2). In the gene network analysis, we observed that TP53 was the hub that controlled cell survival, cell death, and DNA repair in the transgenerational effects of hypoxia through interactions with the BRCA1-interacting protein C-terminal helicase 1 (*BRIP1*), ATP binding cassette subfamily B member 1 (*ABCB1*), and telomerase reverse transcriptase (*TERT*) (Figure 4C). The deregulation of this gene cluster was further validated by qPCR analysis, and the results matched well with the transcriptomic results (Figure 4D). Taken together, our data demonstrated that, similar to the F0 fish in the hypoxia group (F0H), hypoxia also altered the cell cycle and apoptosis in the F2T group, although the F2T group was never exposed to hypoxia. The deregulation of the cell cycle and of apoptotic pathways provides a mechanistic explanation for the transgenerational effects of hypoxia, observed as follicle atresia and altered ovary development.

**Hypoxia Causes Epigenetic Changes in the F2 Transgenerational Group.** DNA methylation is a major epigenetic marker that can be transferred across generations, leading to the transgenerational effects of hypoxia. To test for any changes in DNA methylation patterns caused by hypoxia, reduced representation bisulfite sequencing (RRBS) was conducted. Our result highlighted that exposure of F0 to hypoxia could lead to both hypermethylation and hypomethylation changes in their offspring in the F2 generation (Figure 5A). The CpG methylation changes were distributed primarily in intergenic and exon regions (Figure 5B). We overlaid the results of the transcriptome (DEGs) and methylome (DMRs) analyses of the F2 generation of the transgenerational group to determine the association between gene expression and hypoxia-induced changes in DNA methylation. We found 18 hypomethylated overexpressed genes and 11 hypermethylated suppressed genes (Figure 5C). Gene annotation demonstrated that HS3ST4, LNX2, SPAG1, and ZEB1 were related to cell proliferation and apoptosis. Collectively, our results suggested that hypoxia exposure in the F0 generation could lead to changes in DNA methylation patterns and gene expression levels that are closely related to the observed impairment of oocyte development in the F2 generation of the transgenerational group.

## DISCUSSION

The present study tested the important hypothesis that hypoxia could cause transgenerational reproductive impairment in female fish. Our phenotypic analysis demonstrated that exposure to hypoxia caused two distinct distortions in ovarian development. First, hypoxia could induce follicle atresia, a process that breaks down ovarian follicles through apoptosis.[24] Second, hypoxia led to a significantly greater proportion of primary growth oocytes and significantly fewer vitellogenic oocytes. Furthermore, hatching success was drastically reduced by hypoxia in the F0 generation. Interestingly, similar reproductive impairments were also observed in the F2 generation of the transgenerational group, although they were never exposed to hypoxia. Both follicle atresia and oocyte development are essential processes for egg


DOI: 10.1021/acs.est.8b07250
Environ. Sci. Technol. XXXX, XXX, XXX−XXX

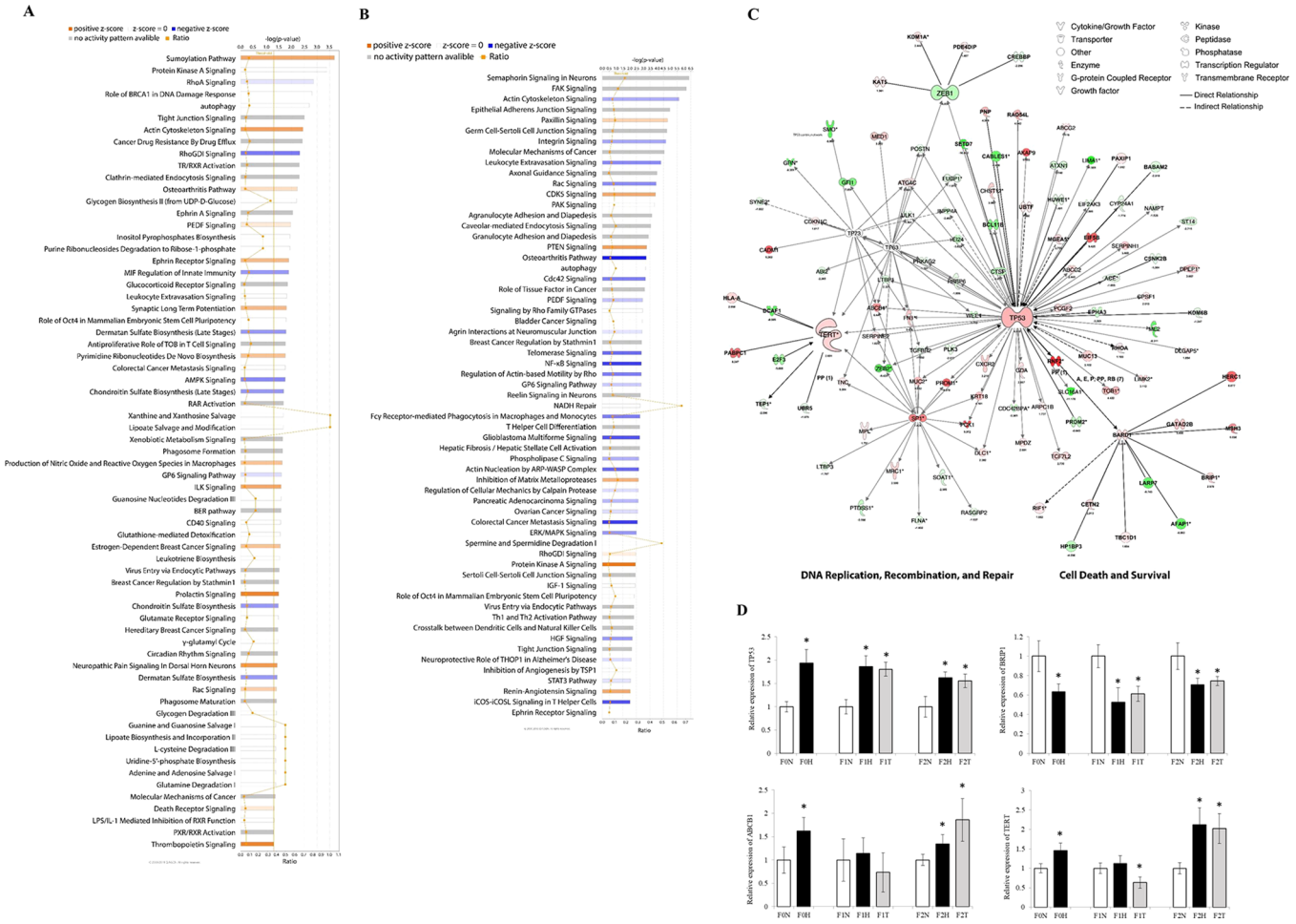


**Figure 4.** Ingenuity pathway analysis (IPA) of differentially expressed genes in ovaries of F0 and F2 generations. Alteration of canonical pathways in the (**A**) F0H and (**B**) F2T groups. The *X*-axis (top) represents −log (*p*-value), and the *x*-axis (bottom) represents the ratio of the number of genes mapped to the total number of genes in the pathway. The *Y*-axis represents canonical pathways. (**C**) Gene regulatory network according to IPA. Red and green colors denote induction and suppression of genes, respectively. The intensity of color represents the degree of differentiation. (**D**) Validation of the differential expression of tumor suppressor protein (*TP53*), BRCA1 interacting protein C-terminal helicase 1 (*BRIP1*), ATP binding cassette subfamily B member 1 (*ABCB1*), and telomerase reverse transcriptase (*TERT*) by qRT-PCR. Data are presented as means ± SEM (*$p < 0.05$, $n = 16$).

production and are closely associated with egg quality.[25,26] The number of mature oocytes was not affected by hypoxia exposure and is consistent with the result that hypoxia has no effect on the fecundity (data not shown). However, the egg quality was adversely affected transgenerationally by hypoxia. In fish, oocyte development is divided into five stages (stage I primary growth stage; stage II cortical alveolus stage; stage III vitellogenesis; stage IV oocyte maturation; and stage V mature egg).[27] It has been reported in mammals that the rate of atresia in follicles is associated with polycystic ovary syndrome (PCOS), which is the most common cause of anovulatory infertility and menstrual cycle abnormalities.[28] Additionally, oogenesis is critically dependent upon correct oocyte−follicle cell interactions,[29] and maturation arrest of oocytes at various stages of the cell cycle can lead to infertility.[30] Here, we have demonstrated that hypoxia can cause transgenerational reproductive impairment in the female germ line. This new piece of evidence, together with our previous findings of transgenerational reproductive impairments in male fish (reduced sperm quality and quantity),[6] indicates that hypoxia can cause transgenerational reproductive impairments in both males and females through different mechanisms and phenotypic changes.

To gain insight into the epigenetic mechanism underlying the observed reproductive impairments, we conducted comparative transcriptomic and methylomic analyses. Our transcriptomic analysis focused on pathways involved in cell cycle control and apoptosis, which are critical to follicle atresia and ovarian development. Our results showed that hypoxia led to the deregulation of a number of canonical pathways related to cell proliferation and cell death in the ovary of the F0 generation, including autophagy, protein kinase A signaling, telomerase signaling, p53 signaling, PEDF signaling, the STAT3 pathway, and FAK signaling. More importantly, deregulation of these important pathways was also observed in the F2 transgenerational group, suggesting that hypoxic stress in the F0 generation could lead to altered signal transduction in the F2 generation. One of the hypoxia-responsive cell signaling pathways is the pigment epithelium-derived factor (PEDF) signaling pathway, which is reported to be suppressed by hypoxic stress, leading to the activation of TP53.[31] In the gene network analysis, TP53 was found to be the hub that controlled both cell-cycle arrest and apoptosis.


DOI: 10.1021/acs.est.8b07250
*Environ. Sci. Technol.* XXXX, XXX, XXX−XXX

**Table 2. Common Deregulated Canonical Pathways in F0H and F2T[a]**

| IPA canonical pathway analysis | F0H | F2T |
|---|---|---|
| autophagy | Autophagy Related 4C Cysteine Peptidase (ATG4C), | Autophagy Related 4C Cysteine Peptidase (ATG4C), |
| | Angiotensin-converting enzyme (ACE), | Angiotensin-converting enzyme (ACE), |
| | Cathepsin Z (CTSZ), | Cathepsin V (CTSV), |
| | Lysosome-associated membrane glycoprotein 2 (LAMP2), | Serine/threonine-protein kinase ULK1 (ULK1), |
| | Cathepsin L (CTSL), | Cathepsin B (CTSB), |
| | Lysosome-associated membrane glycoprotein 1 (LAMP1), | Cathepsin F (CTSF) |
| | Sequestosome-1 (SQSTM1) | |
| role of BRCA1 in DNA damage response | tumor protein p53 (TP53), | tumor protein p53 (TP53), |
| | Beta actin (ACTB), | Beta actin (ACTB), |
| | Transcription factor E2F3 (E2F3), | Transcription factor E2F3 (E2F3), |
| | BRCA1 Interacting Protein C-Terminal Helicase 1 (BRIP1), | BRCA1 Interacting Protein C-Terminal Helicase 1 (BRIP1), |
| | Retinoblastoma 1 (RB1), | Polybromo 1 (PBRM1), |
| | Breast cancer type 1 susceptibility protein homologue (BRCA1), | BRCA1-associated RING domain protein 1 (BARD1), |
| | | BRISC And BRCA1 A Complex Member 2 (BABAM2) |
| PEDF signaling | tumor protein p53 (TP53), | tumor protein p53 (TP53), |
| | Zinc finger E-box-binding homeobox 1 (ZEB1), | Zinc finger E-box-binding homeobox 1 (ZEB1), |
| | Transcription Factor 7 Like 2 (TCF7L2), | Transcription Factor 7 Like 2 (TCF7L2), |
| | Caspase-7 (CASP7), | Phosphatidylinositol-4-Phosphate 3-Kinase Catalytic Subunit Type 2 Beta (PIK3C2B), |
| | proto-oncogene serine/threonine-protein kinase (RAF1), | Ras Homologue Family Member A (RHOA), |
| | Transcription Factor 4 (TCF4), | NFKB Inhibitor Epsilon (NFKBIE) |
| | Ras-related C3 botulinum toxin substrate 1 (RAC1), | |
| | Phosphoinositide-3-Kinase Regulatory Subunit 6 (PIK3R6) | |
| protein kinase A signaling | Receptor-type tyrosine-protein phosphatase kappa (PTPRK), | Receptor-type tyrosine-protein phosphatase kappa (PTPRK), |
| | Protein Tyrosine Phosphatase, Non-Receptor Type 13 (PTPN13), | Protein Tyrosine Phosphatase, Non-Receptor Type 13 (PTPN13), |
| | Protein Tyrosine Phosphatase, Non-Receptor Type 9 (PTPN9), | Protein Tyrosine Phosphatase, Non-Receptor Type 9 (PTPN9), |
| | Anaphase Promoting Complex Subunit 1 (ANAPC1), | Anaphase Promoting Complex Subunit 1 (ANAPC1), |
| | Transforming Growth Factor Beta Receptor 2 (TGFBR2), | Transforming Growth Factor Beta Receptor 2 (TGFBR2), |
| | Filamin-A (FLNA), | Filamin-A (FLNA), |
| | Eyes absent homologue 3 (EYA3), | Eyes absent homologue 3 (EYA3), |
| | Smoothened homologue (SMO), | Smoothened homologue (SMO), |
| | Protein Kinase AMP-Activated Non-Catalytic Subunit Gamma 2 (PRKAG2), | Protein Kinase AMP-Activated Non-Catalytic Subunit Gamma 2 (PRKAG2), |
| | Transcription Factor 7 Like 2 (TCF7L2), | Transcription Factor 7 Like 2 (TCF7L2), |
| | A-Kinase Anchoring Protein 12 (AKAP12), | NFKB Inhibitor Epsilon (NFKBIE), |
| | proto-oncogene serine/threonine-protein kinase (RAF1), | A-kinase anchor protein 9 (AKAP9), |
| | Transcription Factor 4 (TCF4), | CREB Binding Protein (CREBBP), |
| | Inositol 1,4,5-Trisphosphate Receptor Type 1 (ITPR1), | Receptor-type tyrosine-protein phosphatase F (PTPRF), |
| | Nuclear factor of activated T-cells, cytoplasmic 1 (NFATC1), | Glycogen synthase, muscle (GYS1), |
| | Pyruvate Dehydrogenase Kinase 2 (PDK2), | Protein Phosphatase 1 Regulatory Subunit 10 (PPP1R10), |
| | Adenylate cyclase type 9 (ADCY9), | Ras Homologue Family Member A (RHOA), |
| | cAMP-specific 3′,5′-cyclic phosphodiesterase 4D (PDE4D), | cGMP-specific 3′,5′-cyclic phosphodiesterase (PDE5A), |
| | Protein Tyrosine Phosphatase, | Protein Kinase D3 (PRKD3) |
| | Receptor Type R (PTPRR) | |
| RhoGDI signaling | Actin Related Protein2/3Complex Subunit 1B (ARPC1B), | Actin Related Protein2/3Complex Subunit 1B (ARPC1B), |
| | Beta actin (ACTB), | Beta actin (ACTB), |
| | Rho Guanine Nucleotide Exchange Factor 10 (ARHGEF10), | Rho Guanine Nucleotide Exchange Factor 10 (ARHGEF10), |
| | LIM domain kinase 2 (LIMK2), | LIM domain kinase 2 (LIMK2), |
| | Integrin Subunit Beta 1(ITGB1), | Diacylglycerol kinase zeta (DGKZ), |
| | Rho Guanine Nucleotide Exchange Factor 12 (ARHGEF12), | Ras Homologue Family Member A (RHOA), |
| | Rho Guanine Nucleotide Exchange Factor 7 (ARHGEF7), | CREB Binding Protein (CREBBP), |



DOI: 10.1021/acs.est.8b07250
Environ. Sci. Technol. XXXX, XXX, XXX−XXX

**Table 2. continued**

| IPA canonical pathway analysis | F0H | F2T |
|---|---|---|
| | WAS/WASL Interacting Protein Family Member 1 (WASL), | Rho GTPase Activating Protein 35 (ARHGAP35), |
| | Integrin Subunit Alpha 2 (ITGA2), | DLC1 Rho GTPase Activating Protein (DLC1), |
| | Ras-related C3 botulinum toxin substrate 1 (RAC1), | Phosphatidylinositol-5-Phosphate 4-Kinase Type 2 Gamma (PIP4K2C) |
| | Rho-related GTP-binding protein RhoU (RHOU) | |
| RhoA signaling | Beta actin (ACTB), | Beta actin (ACTB), |
| | LIM domain kinase 2 (LIMK2), | LIM domain kinase 2 (LIMK2), |
| | Actin Related Protein2/3Complex Subunit 1B (ARPC1B), | Actin Related Protein2/3Complex Subunit 1B (ARPC1B), |
| | Protein Tyrosine Kinase 2 (PTK2), | Rap Guanine Nucleotide Exchange Factor 2 (RAPGEF2), |
| | Myosin Phosphatase Rho Interacting Protein (MPRIP), | Ras Homologue Family Member A (RHOA), |
| | Rho Guanine Nucleotide Exchange Factor 12 (ARHGEF12), | Citron Rho-Interacting Serine/Threonine Kinase (CIT), |
| | Insulin-like growth factor 1 receptor (IGF1R) | Rho GTPase Activating Protein 35 (ARHGAP35), |
| | | DLC1 Rho GTPase Activating Protein (DLC1), |
| | | Phosphatidylinositol-5-Phosphate 4-Kinase Type 2 Gamma (PIP4K2C) |
| telomerase signaling | tumor protein p53 (TP53), | tumor protein p53 (TP53), |
| | Telomerase reverse transcriptase (TERT), | Telomerase reverse transcriptase (TERT), |
| | Sp1 Transcription Factor (SP1), | Transcription factor Sp1 (SP1), |
| | Retinoblastoma 1 (RB1), | Phosphatidylinositol-4-Phosphate 3-Kinase Catalytic Subunit Type 2 Beta (PIK3C2B), |
| | proto-oncogene serine/threonine-protein kinase (RAF1), | Telomerase protein component 1 (TEP1) |
| | Phosphoinositide-3-Kinase Regulatory Subunit 6 (PIK3R6), | |
| | Tripeptidyl-peptidase 1 (TPP1), | |
| | ETS domain-containing protein Elk-3 (ELK3), | |
| | Protein Phosphatase 2 Regulatory Subunit B'Alpha (PPP2R5A) | |
| p53 signaling | tumor protein p53 (TP53), | tumor protein p53 (TP53), |
| | Retinoblastoma 1 (RB1), | Phosphatidylinositol-4-Phosphate 3-Kinase Catalytic Subunit Type 2 Beta (PIK3C2B), |
| | Thrombospondin 1 (THBS1), | Mediator of RNA polymerase II transcription subunit 1 (MED1), |
| | Protein Phosphatase 1 Regulatory Subunit 13B (PPP1R13B), | Serpin Family E Member 2 (SERPINE2) |
| | Phosphoinositide-3-Kinase Regulatory Subunit 6 (PIK3R6), | |
| | Homeodomain-interacting protein kinase 2 (HIPK2), | |
| | Breast cancer type 1 susceptibility protein homologue (BRCA1) | |
| STAT3 pathway | Transforming Growth Factor Beta Receptor 2 (TGFBR2), | Transforming Growth Factor Beta Receptor 2 (TGFBR2), |
| | Interleukin 10 Receptor Subunit Beta (IL10RB), | Interleukin 10 Receptor Subunit Beta (IL10RB) |
| | proto-oncogene serine/threonine-protein kinase (RAF1), | |
| | Ras-related C3 botulinum toxin substrate 1 (RAC1), | |
| | Insulin-like growth factor 1 receptor (IGF1R), | |
| | Bone morphogenetic protein receptor type-2 (BMPR2), | |
| | Insulin receptor (INSR) | |
| FAK signaling | Beta actin (ACTB), | Beta actin (ACTB), |
| | Talin-1 (TLN1), | Talin-1 (TLN1), |
| | Integrin Subunit Beta 1 (ITGB1), | Phosphatidylinositol-4-Phosphate 3-Kinase Catalytic Subunit Type 2 Beta (PIK3C2B), |
| | proto-oncogene serine/threonine-protein kinase (RAF1), | Breast cancer antiestrogen resistance protein 1 (BCAR1) |
| | Rho Guanine Nucleotide Exchange Factor 7 (ARHGEF7), | |
| | Tyrosine-protein kinase CSK (CSK), | |
| | Integrin Subunit Alpha 2 (ITGA2), | |
| | Ras-related C3 botulinum toxin substrate 1 (RAC1), | |
| | ARF GTPase-activating protein GIT2 (GIT2), | |
| | Protein Tyrosine Kinase 2 (PTK2), | |
| | Calpain 1 (CAPN1), | |
| | Phosphoinositide-3-Kinase Regulatory Subunit 6 (PIK3R6), | |
| | Tensin 1 (TNS1) | |

[a]The common deregulated genes are underlined.



DOI: 10.1021/acs.est.8b07250
Environ. Sci. Technol. XXXX, XXX, XXX−XXX

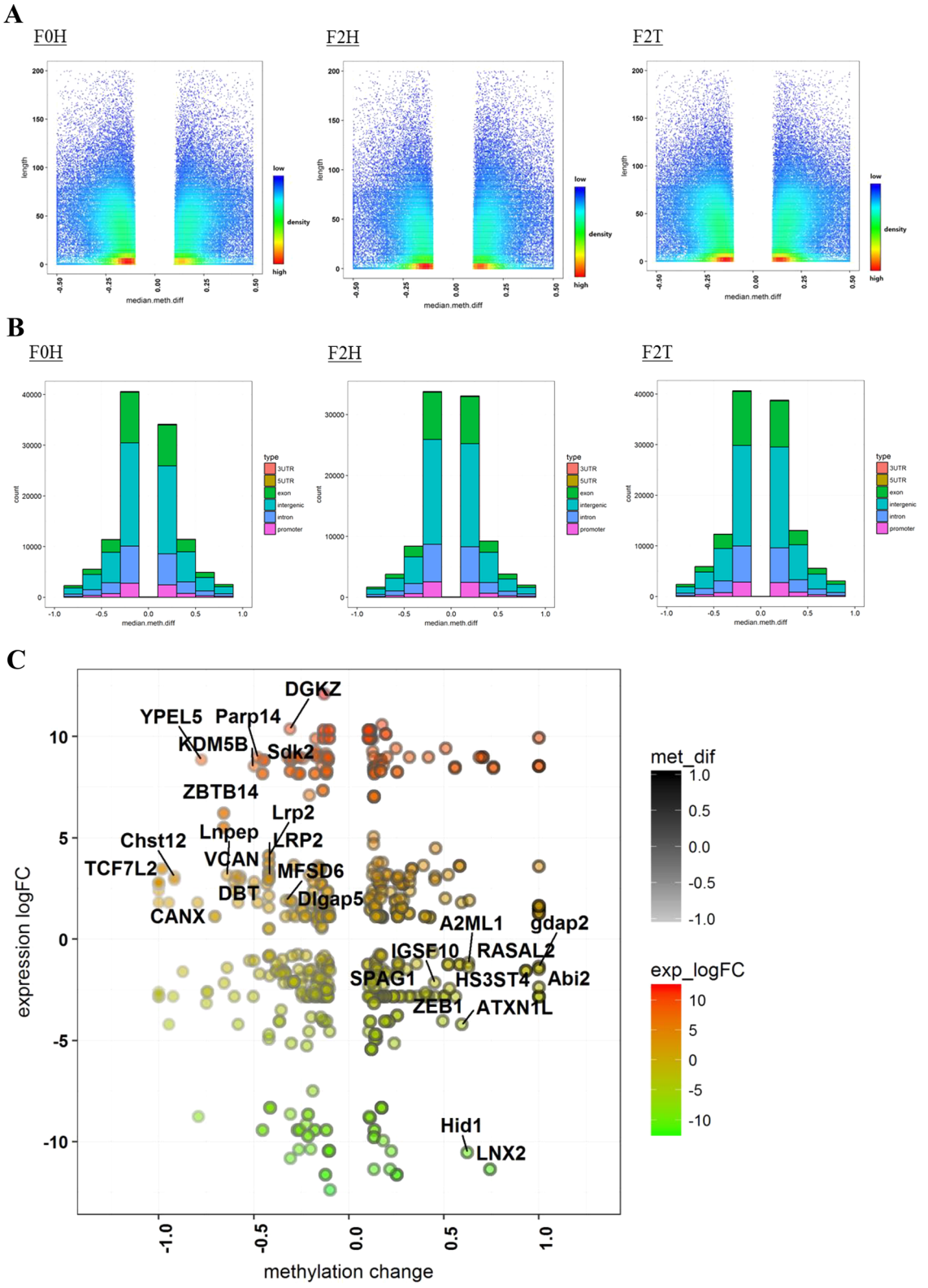


**Figure 5.** Transgenerational effect of hypoxia on the ovarian epigenome. (**A**) Methylation changes in the F2N, F2T, and F2H groups ($n$ = 6). The $X$-axis represents the length of CpG, and the $y$-axis represents methylation changes (negative values indicate hypomethylation; positive values indicate hypermethylation). (**B**) Distribution of differentially methylated regions (DMRs) in the F0H, F2T, and F2H groups compared to the corresponding normoxia group. (**C**) Overlapping of transcriptome and methylome data in the F2 generation of the transgenerational group. The $X$-axis represents the fold change of gene expression (positive values indicate induction; negative values indicate reduction). The $Y$-axis represents methylation change (negative values indicate hypomethylation; positive values indicate hypermethylation).

TP3 also maintained genomic stability through crosstalk with signaling pathways, such as the BRCA1 pathway.[32] It has also been reported that hypoxia can induce TP53 to mediate apoptosis.[33] In our case, the induction of TP53 may serve as a



DOI: 10.1021/acs.est.8b07250
Environ. Sci. Technol. XXXX, XXX, XXX−XXX

defensive response to hypoxia to avoid genome instability. In addition to programmed cell death, hypoxia-induced autophagy is also an important nonapoptotic cell death mechanism,[34] which plays a role in modulating the postmaturation aging of oocytes[35] and establishing the primordial follicle pool.[36] Protein kinase A (PKA) is a cAMP-dependent protein kinase that is known to control various biological processes in the ovary. It has been reported that a high level of PKA activity arrests oocytes in the ovary at prophase during meiosis I.[37] PKA can also mimic the actions of follicle-stimulating hormone (FSH) to promote granulosa cell (GC) differentiation.[38] Liu and Ge[39] demonstrated the role of PKA in estradiol-induced expression of luteinizing hormone receptor in zebrafish ovarian follicle cells. In addition, hypoxia regulates cell proliferation and steroidogenesis through PKA signaling in the bovine corpus luteum,[8] indicating that PKA signaling is essential in ovarian function. Although the sets of deregulated pathways are similar between the F0 hypoxic and F2 transgenerational groups, the immediate and transgenerational effects appear to be controlled by different gene clusters. Notably, other important genes, such as TP53, TERT, and ZEB1 also play key roles in the pathways. Telomerase reverse transcriptase (TERT), the catalytic component of telomerase and the rate-limiting determinant of telomerase activity, is known to be sensitive to environmental stresses, including hypoxia.[40] It has also been reported that the telomere length of blood leukocytes is elongated under mild hypoxia,[41] suggesting that the dissolved oxygen level is critical in determining telomerase activity.

To further elucidate the cause and effect of hypoxia-induced epigenetic modifications, we overlaid the results of the transcriptomic and methylomic analyses of the F2 transgenerational group. We found clusters of hypomethylated induced genes and hypermethylated suppressed genes. These two gene clusters constituted clear signals that transgenerational effects could be transmitted through the inheritance of methylation marks on the genome. Within these two gene clusters, we found some genes that are closely associated with stress-induced apoptosis and cell cycle arrest. For example, zinc finger E-box-binding homeobox 1 (ZEB1) is a transcription factor that is frequently deregulated in various cancers, leading to altered cell proliferation.[42] Interestingly, ZEB1 is a downstream effector of TP53,[43] indicating that the effects of hypoxia-induced TP53 expression may be mediated by epigenetic regulation of ZEB1. However, this proposed mechanism remains to be confirmed. Additionally, ZEB1 is associated with TERT in controlling cell growth and apoptosis,[44] suggesting the importance of TP53-TERT-ZEB1 complexes in oocyte development. Sperm-associated antigen 1 (SPAG1) was found to be suppressed and under hypermethylation in the F2 generation of the transgenerational group. SPAG1 is a novel microtubule-associated protein that plays a key role in oocyte meiosis. Progression through the G2/M phase was compromised in SPAG1-depleted oocytes.[45] There are also numerous deregulated genes, such as TP53 and TERT that were not controlled by DNA methylation. The transgenerational alteration of TP53 can also be mediated by other epigenetic modifications, such as histone modification or miRNA. The other possible indirect mechanism is epigenetic modification on the upstream mediator of TP53. For example, hepatoma upregulated protein (HURP), which was observed to be hypomethylated, could be associated with the deregulation of ATM and TP53.[46] Thus, the transgenerational effects caused by hypoxia can arise through various alterations in cell signaling.

Intriguingly, when we compared the results of the current study in female fish with our previous study in male fish,[6] it is observed that the maternal and paternal transgenerational effects in response to hypoxia, especially the core hub of the altered pathway, are different. In the analysis of data from male fish, the impairment of sperm quality was mainly mediated by euchromatic histone lysine methyltransferase 2 (EHMT2), which is a methyltransferase that methylates the lysine residues of histone H3. However, in female fish, the major regulator in the observed impairment of ovarian development is TP53. Although the underlying mechanisms of reproductive impairment are sex-specific, our results demonstrated that the transgenerational effect of hypoxia on both males and females is similarly controlled by DNA methylation.

This report demonstrates that exposure to hypoxia in F0 leads to follicle atresia and alters oocyte development in the F2 generation via relevant DNA methylation and transcriptomic changes. This, together with the transgenerational reproductive impairments previously reported in male fish exposed to hypoxia, indicates that hypoxia, which occurs over large areas in our freshwater and marine environments, may pose a significant and long lasting threat to the sustainability of natural fish populations worldwide. As transgenerational effects may be reversible[47,48] a further study on F3 and F4 generations could provide a better understanding of the duration of the transgenerational effect caused by hypoxia.

## ■ ASSOCIATED CONTENT

### Supporting Information

The Supporting Information is available free of charge on the ACS Publications website at DOI: 10.1021/acs.est.8b07250.

Supplementary Data Set S1 (XLSX)
Supplementary Data Set S2 (XLSX)
Supplementary Data Set S3 (XLSX)
Supplementary Data Set S4 (XLSX)
Supplementary Data Set S5 (XLSX)
Supplementary Data Set S6 (XLSX)
Supplementary Data Set S7 (XLSX)
Supplementary Data Set S8 (XLSX)
Stages (primary growth oocytes, vitellogenic oocytes, and mature oocytes) of oocyte development in F0 and F2 generations (F0 $n = 6$; F2 $n = 7$). Asterisks denote statistical significance relative to the normoxic group (*$p < 0.05$). Representative histological images of hematoxylin and eosin staining in F0 and F2 generations (20×). Primary-stage oocytes are circled with dotted lines; mature oocytes are indicated with asterisks (PPTX)

### Accession Codes

Sequencing data of transcriptome sequencing and reduced representation bisulfite sequencing that support the findings of this study have been deposited in the NCBI Sequence Read Archive (SRA) (http://www.ncbi.nlm.nih.gov/sra) with the accession codes **SRP150111** and **SRP144928**, respectively.

## ■ AUTHOR INFORMATION

### Corresponding Author

*Mailing address: Department of Science and Environmental Studies, The Education University of Hong Kong, Hong Kong SAR, China. Email address: rudolfwu@eduhk.hk.



DOI: 10.1021/acs.est.8b07250
Environ. Sci. Technol. XXXX, XXX, XXX−XXX

### ORCID

Simon Yuan Wang: 0000-0002-9089-2617
Jae-Seong Lee: 0000-0003-0944-5172
Rudolf Shiu Sun Wu: 0000-0002-8865-8709


### Author Contributions

^These authors contributed equally to this work. K.P.L. and S.Y.W. participated in sample preparation, sequencing, and drafted the manuscript; J.W.L., N.J., Y.T., B.Y.L., J.S.L., J.W.Z., and T.F.C. carried out the sequencing data analysis and drafted the manuscript; S.Y.W., N.T., and A.T. designed the experiment, carried out the exposure experiment, and collected the samples; A.S.T.W., D.W.T.A., and M.T.W. participated in immunohistochemistry and performed the statistical analysis; R.S.S.W. conceived the idea and formulated the hypothesis; R.S.S.W. and R.Y.C.K. designed the experiment and helped to draft the manuscript. All authors have read and approved the final manuscript.

### Notes

Ethics approval and consent to participate. All animal research procedures were approved by the Committee on the Use of Live Animals in Teaching and Research (CULATR, no. 2714-12) at the University of Hong Kong.
The authors declare no competing financial interest.

## ■ ACKNOWLEDGMENTS

We thank Michael Chiang for designing the schematic diagram. This work was supported in part by a grant from the National Natural Science Foundation of China (Project 21577114) to RYCK, an Area of Excellence grant (AoE/P-04/04) from the University Grants Committee, and a grant from the State Key of Marine Pollution awarded to R.S.S.W. T.F.C. is in part supported by a General Research Fund (14102014) from the Research Grants Council of the Hong Kong government. This work was supported by the State Key Laboratory of Marine Pollution (SKLMP) Seed Collaborative Research Fund granted to K.P.L.

## ■ REFERENCES


(1) Diaz, R. J.; Rosenberg, R. Spreading dead zones and consequences for marine ecosystems. *Science* **2008**, *321* (5891), 926−929.
(2) Wu, R. S. S. Effects of hypoxia on fish reproduction and development. *Fish Physiology* **2009**, *27*, 79−141.
(3) Altieri, A. H.; Gedan, K. B. Climate change and dead zones. *Global Change Biology.* **2015**, *21*, 1395−1406.
(4) Thomas, P.; Rahman, M. S.; Khan, I. A.; Kummer, J. A. Widespread endocrine disruption and reproductive impairment in an estuarine fish population exposed to seasonal hypoxia. *Proc. R. Soc. London, Ser. B* **2007**, *274* (1626), 2693−2701.
(5) Thomas, P.; Rahman, M. S. Extensive reproductive disruption, ovarian masculinization and aromatase suppression in Atlantic croaker in the northern Gulf of Mexico hypoxic zone. *Proc. R. Soc. London, Ser. B* **2012**, *279* (1726), 28−38.
(6) Wang, S. Y.; Lau, K.; Lai, K. P.; Zhang, J. W.; Tse, A. C.; Li, J. W.; Tong, Y.; Chan, T. F.; Wong, C. K.; Chiu, J. M.; Au, D. W.; Wong, A. S.; Kong, R. Y.; Wu, R. S. S. Hypoxia causes transgenerational impairments in reproduction of fish. *Nat. Commun.* **2016**, *7*, 12114.
(7) Lai, K. P.; Li, J. W.; Tse, A. C.; Chan, T. F.; Wu, R. S. S. Hypoxia alters steroidogenesis in female marine medaka through miRNAs regulation. *Aquat. Toxicol.* **2016**, *172*, 1−8.
(8) Jiang, Y. F.; Tsui, K. H.; Wang, P. H.; Lin, C. W.; Wang, J. Y.; Hsu, M. C.; Chen, Y. C.; Chiu, C. H. Hypoxia regulates cell proliferation and steroidogenesis through protein kinase A signaling in bovine corpus luteum. *Anim. Reprod. Sci.* **2011**, *129*, 152−161.
(9) Shang, E. H.; Wu, R. S. S. Aquatic hypoxia is a teratogen and affects fish embryonic development. *Environ. Sci. Technol.* **2004**, *38*, 4763−4767.
(10) Matthews, S. G.; Phillips, D. I. Transgenerational inheritance of stress pathology. *Exp. Neurol.* **2012**, *233*, 95−101.
(11) Skinner, M. K. Environmental stress and epigenetic transgenerational inheritance. *BMC Med.* **2014**, *12*, 153.
(12) Anway, M. D.; Cupp, A. S.; Uzumcu, M.; Skinner, M. K. Epigenetic transgenerational actions of endocrine disruptors and male fertility. *Science* **2005**, *308*, 1466−1469.
(13) Ben Maamar, M.; Sadler-Riggleman, I.; Beck, D.; Skinner, M. K. Epigenetic transgenerational inheritance of altered sperm histone retention sites. *Sci. Rep.* **2018**, *8*, 5308.
(14) Mennigen, J. A.; Thompson, L. M.; Bell, M.; Tellez Santos, M.; Gore, A. C. Transgenerational effects of polychlorinated biphenyls: 1. Development and physiology across 3 generations of rats. *Environ. Health* **2018**, *17*, 18.
(15) Kurokawa, H.; Aoki, Y.; Nakamura, S.; Ebe, Y.; Kobayashi, D.; Tanaka, M. Time-lapse analysis reveals different modes of primordial germ cell migration in the medaka Oryzias latipes. *Dev., Growth Differ.* **2006**, *48*, 209−221.
(16) Lai, K. P.; Li, J. W.; Wang, S. Y.; Chiu, J. M.; Tse, A.; Lau, K.; Lok, S.; Au, D. W.; Tse, W. K.; Wong, C. K.; Chan, T. F.; Kong, R. Y.; Wu, R. S. S. Tissue-specific transcriptome assemblies of the marine medaka Oryzias melastigma and comparative analysis with the freshwater medaka Oryzias latipes. *BMC Genomics* **2015**, *16*, 135.
(17) Bray, N. L.; Pimentel, H.; Melsted, P.; Pachter, L. Near-optimal probabilistic RNA-seq quantification. *Nat. Biotechnol.* **2016**, *34*, 525−527.
(18) Robinson, M. D.; McCarthy, D. J.; Smyth, G. K. edgeR: a Bioconductor package for differential expression analysis of digital gene expression data. *Bioinformatics* **2010**, *26*, 139−140.
(19) Olova, N.; Krueger, F.; Andrews, S.; Oxley, D.; Berrens, R. V.; Branco, M. R.; Reik, W. Comparison of whole-genome bisulfite sequencing library preparation strategies identifies sources of biases affecting DNA methylation data. *Genome Biol.* **2018**, *19*, 33.
(20) Peat, J. R.; Dean, W.; Clark, S. J.; Krueger, F.; Smallwood, S. A.; Ficz, G.; Kim, J. K.; Marioni, J. C.; Hore, T. A.; Reik, W. Genome-wide Bisulfite Sequencing in Zygotes Identifies Demethylation Targets and Maps the Contribution of TET3 Oxidation. *Cell Rep.* **2014**, *9* (6), 1990−2000.
(21) Kong, R. Y.; Giesy, J. P.; Wu, R. S. S.; Chen, E. X.; Chiang, M. W.; Lim, P. L.; Yuen, B. B.; Yip, B. W.; Mok, H. O.; Au, D. W. Development of a marine fish model for studying in vivo molecular responses in ecotoxicology. *Aquat. Toxicol.* **2008**, *86*, 131−141.
(22) Blazer, V. S. Histopathological assessment of gonadal tissue in wild fishes. *Fish Physiol. Biochem.* **2002**, *26*, 85−101.
(23) Kinoshita, M.; Murata, K.; Naruse, K.; Tanaka, M. *Medaka: biology, management, and experimental protocols*; John Wiley & Sons, 2009.
(24) Lubzens, E.; Young, G.; Bobe, J.; Cerdà, J. Oogenesis in teleosts: how eggs are formed. *Gen. Comp. Endocrinol.* **2010**, *165* (3), 367−389.
(25) Mermillod, P.; Dalbis-Tran, R.; Uzbekova, S.; Thlie, A.; Traverso, J. M.; Perreau, C.; Papillier, P.; Monget, P. Factors affecting oocyte quality: who is driving the follicle? *Reprod. Domest. Anim.* **2008**, *43*, 393−400.
(26) Sirard, M. A. Follicle environment and quality of in vitro matured oocytes. *J. Assist. Reprod. Genet.* **2011**, *28*, 483−488.
(27) Selman, K.; Wallace, R. A.; Sarka, A.; Qi, X. Stages of oocyte development in the zebrafish, Brachydanio rerio. *J. Morphol.* **1993**, *218*, 203−224.
(28) Franks, S.; Stark, J.; Hardy, K. Follicle dynamics and anovulation in polycystic ovary syndrome. *Hum. Reprod. Update* **2008**, *14*, 367−378.



DOI: 10.1021/acs.est.8b07250
*Environ. Sci. Technol.* XXXX, XXX, XXX−XXX

(29) Mtango, N. R.; Potireddy, S.; Latham, K. E. Oocyte quality and maternal control of development. *Int. Rev. Cell Mol. Biol.* **2008**, *268*, 223−290.
(30) Levran, D.; Farhi, J.; Nahum, H.; Glezerman, M.; Weissman, A. Maturation arrest of human oocytes as a cause of infertility: case report. *Hum. Reprod.* **2002**, *17*, 1604−1609.
(31) Gao, G.; Li, Y.; Gee, S.; Dudley, A.; Fant, J.; Crosson, C.; Ma, J. X. Down-regulation of vascular endothelial growth factor and up-regulation of pigment epithelium-derived factor: a possible mechanism for the anti-angiogenic activity of plasminogen kringle 5. *J. Biol. Chem.* **2002**, *277*, 9492−9497.
(32) Arizti, P.; Fang, L.; Park, I.; Yin, Y.; Solomon, E.; Ouchi, T.; Aaronson, S. A.; Lee, S. W. Tumor suppressor p53 is required to modulate BRCA1 expression. *Mol. Cell. Biol.* **2000**, *20*, 7450−7459.
(33) Leszczynska, K. B.; Foskolou, I. P.; Abraham, A. G.; Anbalagan, S.; Tellier, C.; Haider, S.; Span, P. N.; O'Neill, E. E.; Buffa, F. M.; Hammond, E. M. Hypoxia-induced p53 modulates both apoptosis and radiosensitivity via AKT. *J. Clin. Invest.* **2015**, *125*, 2385−2398.
(34) Baehrecke, E. H. Autophagy: dual roles in life and death? *Nat. Rev. Mol. Cell Biol.* **2005**, *6*, 505−510.
(35) Lin, F. H.; Zhang, W. L.; Li, H.; Tian, X. D.; Zhang, J.; Li, X.; Li, C. Y.; Tan, J. H. Role of autophagy in modulating post-maturation aging of mouse oocytes. *Cell Death Dis.* **2018**, *9*, 308.
(36) Sun, Y. C.; Wang, Y. Y.; Sun, X. F.; Cheng, S. F.; Li, L.; Zhao, Y.; Shen, W.; Chen, H. The role of autophagy during murine primordial follicle assembly. *Aging* **2018**, *10*, 197−211.
(37) Duncan, F. E.; Padilla-Banks, E.; Bernhardt, M. L.; Ord, T. S.; Jefferson, W. N.; Moss, S. B.; Williams, C. J. Transducin-like enhancer of split-6 (TLE6) is a substrate of protein kinase A activity during mouse oocyte maturation. *Biol. Reprod.* **2014**, *90*, 63.
(38) Law, N. C.; Donaubauer, E. M.; Zeleznik, A. J.; Hunzicker-Dunn, M. How protein kinase A activates canonical tyrosine kinase signaling pathways to promote granulosa cell differentiation. *Endocrinology* **2017**, *158*, 2043−2051.
(39) Liu, K. C.; Ge, W. Evidence for gating roles of protein kinase A and protein kinase C in estradiol-induced luteinizing hormone receptor (lhcgr) expression in zebrafish ovarian follicle cells. *PLoS One* **2013**, *8* (5), No. e62524.
(40) Peterson, D. R.; Mok, H. O.; Au, D. W. Modulation of telomerase activity in fish muscle by biological and environmental factors. *Comp. Biochem. Physiol., Part C: Toxicol. Pharmacol.* **2015**, *178*, 51−59.
(41) Wang, Y.; Zhou, W. D.; Yang, Y.; Ma, L.; Zhao, Y.; Bai, Z.; Ge, R. L. Telomeres are elongated in rats exposed to moderate altitude. *J. Physiol. Anthropol.* **2014**, *33*, 19.
(42) Caramel, J.; Ligier, M.; Puisieux, A. Pleiotropic roles for ZEB1 in cancer. *Cancer Res.* **2018**, *78*, 30−35.
(43) Ohashi, S.; Natsuizaka, M.; Wong, G. S.; Michaylira, C. Z.; Grugan, K. D.; Stairs, D. B.; Kalabis, J.; Vega, M. E.; Kalman, R. A.; Nakagawa, M.; Klein-Szanto, A. J.; Herlyn, M.; Diehl, J. A.; Rustgi, A. K.; Nakagawa, H. Epidermal growth factor receptor and mutant p53 expand an esophageal cellular subpopulation capable of epithelial-to-mesenchymal transition through ZEB transcription factors. *Cancer Res.* **2010**, *70*, 4174−4184.
(44) Yu, P.; Shen, X.; Yang, W.; Zhang, Y.; Liu, C.; Huang, T. ZEB1 stimulates breast cancer growth by up-regulating hTERT expression. *Biochem. Biophys. Res. Commun.* **2018**, *495*, 2505−2511.
(45) Huang, C.; Wu, D.; Khan, F. A.; Jiao, X.; Guan, K.; Huo, L. The GTPase SPAG-1 orchestrates meiotic program by dictating meiotic resumption and cytoskeleton architecture in mouse oocytes. *Mol. Biol. Cell* **2016**, *27*, 1776−1785.
(46) Hassan, M.; El Khattouti, A.; Ejaeidi, A.; Ma, T.; Day, W. A.; Espinoza, I.; Vijayakumar, S.; Gomez, C. R. Elevated expression of hepatoma up-regulated protein inhibits $\gamma$-irradiation-induced apoptosis of prostate cancer cells. *J. Cell. Biochem.* **2016**, *117*, 1308−1318.
(47) Corrales, J.; Fang, X.; Thornton, C.; Mei, W.; Barbazuk, W. B.; Duke, M.; Scheffler, B. E.; Willett, K. L. Effects on specific promoter DNA methylation in zebrafish embryos and larvae following benzo[a]pyrene exposure. *Comp. Biochem. Physiol., Part C: Toxicol. Pharmacol.* **2014**, *163*, 37−46.
(48) Burggren, W. W. Dynamics of epigenetic phenomena: intergenerational and intragenerational phenotype 'washout'. *J. Exp. Biol.* **2015**, *218* (Pt 1), 80−87.


DOI: 10.1021/acs.est.8b07250
*Environ. Sci. Technol.* XXXX, XXX, XXX−XXX